Engineering Structures 145 (2017) 246–253

Contents lists available at ScienceDirect

Engineering Structures

journal homepage: www.elsevier.com/locate/engstruct

Rigid-foldable tubular arches

Joseph M. Gattas [a], Weilin Lv [b], Yan Chen [c,*]

[a] School of Civil Engineering, University of Queensland, St Lucia QLD 4072, Australia
[b] Key Laboratory of Mechanism and Equipment Design of Ministry of Education, Tianjin University, Tianjin 300072, China
[c] School of Mechanical Engineering, Tianjin University, Tianjin 300072, China

ARTICLE INFO

Article history:
Received 26 October 2016
Revised 1 March 2017
Accepted 19 April 2017

Keywords:
Rigid origami
Miura-ori
Deployable structure
Tubular arches

ABSTRACT

Several types of tubular, origami-inspired plate mechanisms have been proposed for use as meta-materials and deployable structures. However, research into mechanical properties of these mechanisms is limited to rectilinear forms. This paper investigates the structural feasibility of non-rectilinear rigid-foldable cellular materials for application as deployable arch structures. An experimental and numerical investigation is first conducted on a new type of folded tubular arch, with failure contributions identified from hinge rotation and plate buckling failure mechanisms. A common geometric description is then developed between three different types of origami-inspired tubular arches, which are numerically investigated under three-point loading. The double-kite arch developed in this paper is seen to have the highest failure load.

1. Introduction

The Miura-ori is a famous origami pattern with a single degree-of-freedom (DOF) rigid-foldable mechanism [1,2]. Rigid-foldable patterns can fold component panels about crease lines without twisting or stretching. They are therefore widely used in origami-inspired engineering designs [3–8]. Several types of rigid-foldable, rectilinear tubular plate mechanisms have been proposed based on tessellations of the Miura pattern. A multi-layered Miura-ori structure was developed in [9] with outer *face* layers of zero height constraining a partially-folded *core* layer, shown in Fig.1. Miura patterns with different heights have the same in-plane kinematic expansion and so assembly can still fold with 1DOF. A modified version of this configuration was presented in [10] whereby a single-span of the face layer bridged a double-span of the core layer, shown in Fig. 1b. The 1DOF mechanism is preserved and a 'locking' capacity is introduced whereby face hinge lines can attach to core ridges to form a stable structure once deployed. The above two forms are termed single and double-span *morphing sandwich structures* (MSS), respectively. Another form consists of mirrored Miura-ori patterns attached to create a polyhedral cylindrical tube pattern [11], shown in Fig. 1c.

The basic tubular forms have been extended to generate many new types of rigid foldable, space-filling cellular meta-materials [12,9,13]. These use a variety of design methods for mechanism synthesis, for example through coupling of rigid-foldable tubes [14], stacking of congruent tessellations [15], or exploration of compatibility conditions derived from spherical linkage theory [16]. Research into the mechanical properties of these materials is underdeveloped in comparison to research into their geometric behaviours, despite novel mechanics often being a proviso for development of meta-material kinematics. Existing studies are predominantly focused on the mechanical properties of linear cellular forms, including the performance of tubular forms under axial compression [17,18] and out-of-plane loading [19], the performance of stacked Miura-core beams [20,21], and mechanical modelling of the orthotropic behaviour of cellular materials under compression, bending, and shear [22,14].

This paper investigates the structural feasibility of non-rectilinear rigid-foldable cellular materials for application as deployable arch structures. Section 2 first conducts an experimental investigation on a new type of tubular arch under three-point loading. Observed failure modes and force-displacement responses are then used to validate a numerical model in Section 3. A systematic investigation of different types of tubular rigid-foldable arch forms is then undertaken in Section 4, including development of a consistent geometric parametrisation between different types and a numerical investigation of their relative structural performance.

2. Experimental investigation

2.1. Geometric design

As a first step to understanding the behaviour of rigid-foldable tubular arch structures, an experimental investigation was

* Corresponding author.
E-mail address: yan_chen@tju.edu.cn (Y. Chen).

http://dx.doi.org/10.1016/j.engstruct.2017.04.037
0141-0296/

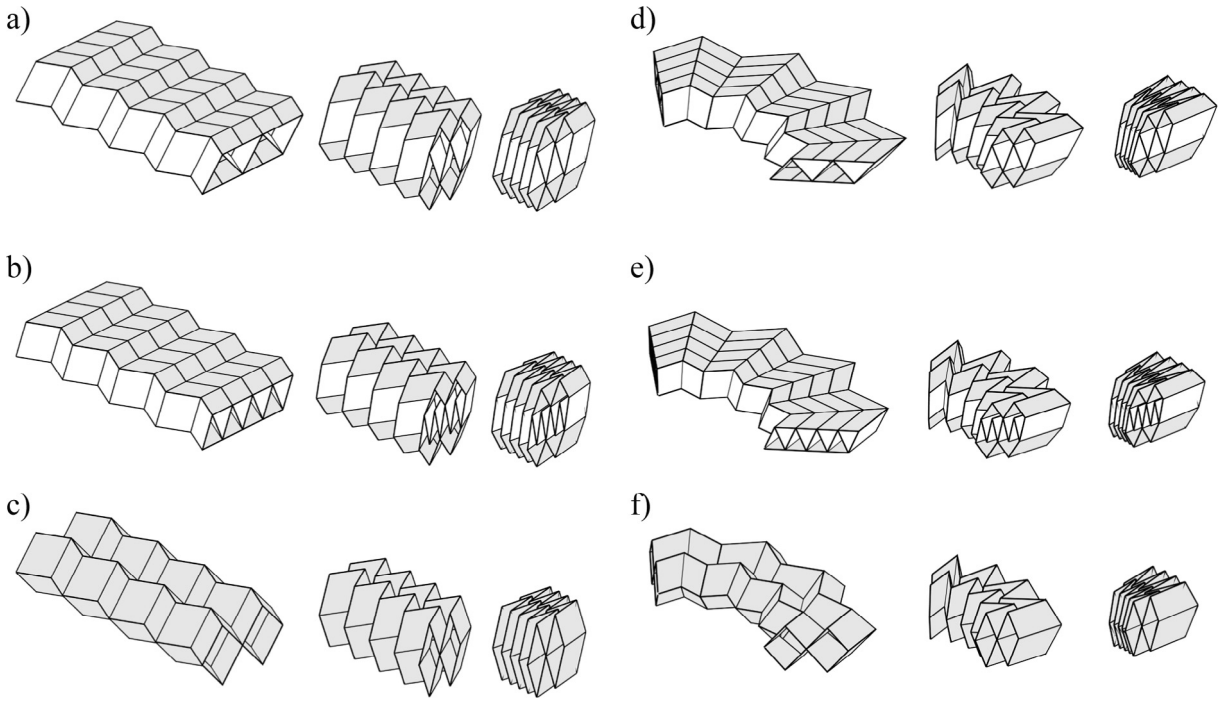

Fig. 1. In-plane tessellations of rectilinear $x-y$ (on left) and polar $r-\theta$ (on right) rigid-foldable tubular structures. a) and d) Single-span MSS. b) and e) Double-span MSS. c) Polyhedral cylindrical tube and f) kite arch.

conducted on a single arch geometry. The arch structure studied in this paper is obtained from the basic 1DOF kite-shaped tube geometry first proposed in [16]. The basic kite-shaped unit is shown in Fig. 2a and consists of two folded sheet layers, one white and one grey, which are joined at the ridge lines. Each is composed of four identical parallelograms with side lengths l_1 and l_2, where $l_1 > l_2$. To achieve a flat foldability condition as shown in Fig. 2b, the following condition must be satisfied

$$l_1 \cos\alpha_1 = l_2 \cos\alpha_2 \tag{1}$$

where α_1 and α_2 are parallelogram sector angles. A third sheet layer, identical to the grey one in Section 2a, is added to form a three-piece unit which can be considered as two kite-shaped units merged together. The assembly is termed a *double-kite* unit and is shown in Section 2c. When the central white layer is fully-deployed to a flat condition, the unit reaches its working state, at which point the dihedral angle θ in grey layers becomes

$$\cos\theta = \frac{l_1^2(1+\cos^2\alpha_1) - 2l_2^2}{l_1^2 \sin^2\alpha_1} \tag{2}$$

In order to form an arch profile, two ends of the double-kite unit are modified by truncation with two planes that are inclined at angle η to the middle plane, as shown in Section 2d. The parallelogram facets then become trapezoidal. When the inner white layer is fully deployed into a flat piece, the following relationship can be derived

$$R = \sin\alpha_2 \left(\frac{l_R}{\sin\eta} - \frac{l_2}{\sin(\alpha_2+\eta)} \right) \tag{3}$$

The outer layer, shown in grey in Fig. 2e, will then have the geometric relationship

$$\cot\beta = -\frac{l_2 \sin\alpha_2 \cot(\alpha_2+\eta)}{l_1 \sin\alpha_1} \tag{4}$$

These units can tessellate to form a *double-kite arch*, with an eight unit arch shown in Fig. 2f-g. If eight units tessellate to form a semi-circle, η can be obtained as $\pi/16 = 11.25°$. Four additional parameters then need be specified, for example $R = 120$ mm, $\alpha_2 = 52.14°, l_1 = 31.83$ mm, and $l_2 = 21.87$ mm, with the four remaining parameters obtainable from and Eqs. (1)–(4) as $\alpha_1 = 64.74°, \theta = 73.34°, l_R = 34.63$ mm, and $\beta = 106.57°$.

2.2. Manufacture and assembly

A prototype arch was designed with the above geometric specification and manufactured from 0.3 mm thick EnDURO Ice polyvinyl chloride (PVC) coated sheets. A Silhouette CAMEO electronic cutting tool was used to manufacture the crease pattern, with internal creases lightly scored and external boundaries through-cut. Outside layer and inside layer crease patterns are shown in Fig. 3a-b, a-b, respectively. A series of assembly methods were trialled until one was found that produced repeatable results. First, parts for each layer of the tube were manufactured with external tabs added to the inside layer and one of the outer layer crease patterns. Second, each layer was separately folded along crease lines to ensure correct polarity when assembled. Third, tabs were glued between inner-outer and outer-outer layers with Aibida 502 adhesive. The final assembled prototype is shown in elevation and isometric in Fig. 3c-d, c-d, in top view in Fig. 3e with glued tabs highlighted, and in section in Fig. 3f with core layer highlighted.

2.3. Testing method

Three arch samples were tested on an Intron 5982. The test configuration is shown in Fig. 4a, with the arch fixed at each end by a 3D printed support and loaded centrally by a 60 mm by 80 mm rigid top plate. A 100 N load cell was sufficient for the test, with an internal Instron load cell used and force and displacement values measured from Intron cross head. A controlled-displacement loading was applied at 12 mm/minute until a maximum displacement of 120 mm was reached. The measured force-displacement responses are shown in Fig. 4b. Good consistency is seen between